Journal of Marine Science and Technology (2019) 24:111–122
https://doi.org/10.1007/s00773-018-0535-5

ORIGINAL ARTICLE

Experimental investigation of rotating cylinders in flow

Wei Chen[1] · **Chang-Kyu Rheem**[1]

Received: 19 April 2017 / Accepted: 24 December 2017 / Published online: 9 February 2018

Abstract
Rotating cylinders with different diameters placed in uniform flow were investigated experimentally. The aspect ratios, AS (ratio of the length and the diameter) of cylinders, with the same length $L = 0.59$ m were 1.85, 2.21, 2.73 and 5.78 with respective diameters of 0.319, 0.267, 0.216 and 0.102 m. The non-dimensional rotation rate, α, was the ratio of the rotating surface speed and the flow speed, which varied from 0 to 8 for the 0.319 m diameter cylinder. Hydrodynamics of the cylinders were analyzed based on two different conditions: cylinders in flow condition and rotating cylinders in flow condition. For the cylinders in flow, the influence of the aspect ratio and Reynolds number on the hydrodynamics coefficient and Strouhal number was discussed, the critical transition area was found at $1.0 \times 10^5 \leqslant Re \leqslant 1.59 \times 10^5$. For the cylinders rotating in flow, initial area, increasing area and equivalent area were defined to describe the variation of mean of hydrodynamics as the increase of rotation rates. The range of these areas was decided by the rotation rate and aspect ratio of the cylinders. Different from the mean hydrodynamics, for the Strouhal number (vortex shedding) and Root mean square of lift for the rotating cylinders, vortex shedding area, weak vortex shedding area and wake fluctuation area were defined to explain them and the range of these areas was only determined by rotation rate.

Keywords Rotating cylinder · Aspect ratio · Rotation rate · Hydrodynamics

1 Introduction

Flow past linear structures has been investigated by many researchers, including the research conducted by Feng [1] to investigate the cross flow oscillation at Reynolds numbers between 10,000 and 50,000. The lock-in phenomenon of a spring-mounted cylinder occurred at reduced velocity range 5–7 is presented in his research. However, the condition is more difficult for rotating cylinders in flow. Prandtl [2] conducted one of the earliest experiments; his results suggested that the maximum lift generated by a rotating cylinder in uniform flow is limited to 4π. The effect of end conditions and aspect ratio were presented in his research. Prandtl and Tietjens [3] carried out experiments to investigate complex flow fields, but it was difficult to measure pressure distribution because of the rotation and limitation of experimental equipment. Swanson [4] solved the pressure measurement problem by detecting the lift and drag force directly, his results indicated a pronounced Reynolds number dependence of lift and drag forces existed in the region where the rotation rate α was smaller than 1. Chew [5] used a single pressure transducer with mercury slip ring and the ensemble-averaging technique to measure the pressure around a rotating cylinder; his results indicated a shift in mean separation locations in the direction of rotation, shift in stagnation location against the direction of rotation and asymmetry of mean pressure distribution around the cylinder that induced increase of lift force. Since then, many studies have been conducted on this issue [6–12].

One interesting question is whether Prandtl's limit can be exceeded; Prandtl suggested that the maximum mean lift generated by a rotating cylinder placed in uniform flow is 4π, as shown in Fig. 1. Tokumaru and Dimotakis [13] devised a method based on an inviscid point-vortex method and their results indicated that Prandtl's limit could be exceeded; they estimated that the lift force coefficient at $\alpha = 10$ is more than 20% larger than this limit. Chew et al. [9] computed the lift for $0 \leqslant \alpha \leqslant 6$ at $Re = 100$, their results were in agreement with Prandtl's postulate and a mean lift coefficient of 9.1 was predicted at $\alpha = 6$. Mittal and Kumar [11] used a two-dimensional computation method to investigate the flow past

✉ Wei Chen
chenwei@iis.u-tokyo.ac.jp

[1] Department of Ocean Technology, Policy and Environment, University of Tokyo, Tokyo 1538505, Japan

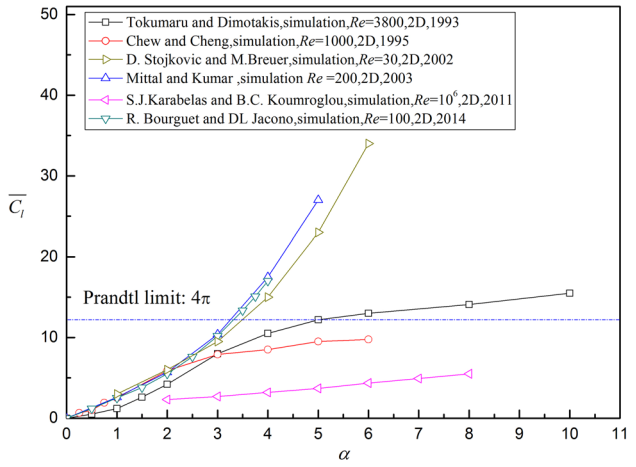

Fig. 1 Mean Lift coefficient, $\overline{C}_l$, versus rotation rate, α, from previous works (2D = two-dimensional)

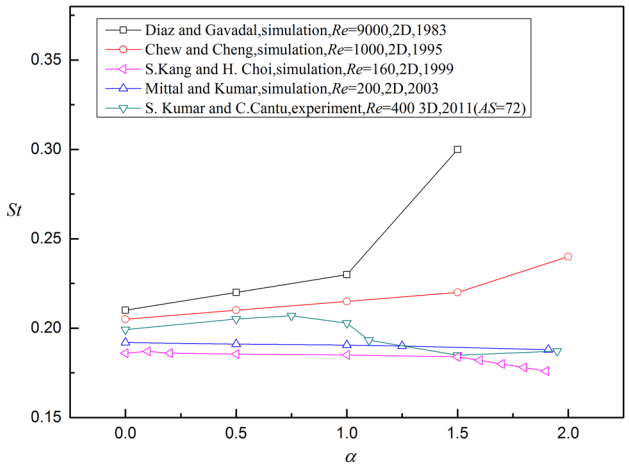

Fig. 2 Strouhal number, *St*, versus rotation rate, α, from previous works (*AS* aspect ratio)

a rotating cylinder at $0 \leqslant \alpha \leqslant 5$ and the lift at $\alpha = 5$ reached 27, which is much larger than the Prandtl's limit; they concluded that very large lift coefficients can be obtained due to the Magnus effect for large rotation rates. Bourguet and Lo Jacono [14] investigated the lift of a rotating cylinder at $Re = 100$ based on two- and three-dimensional numerical simulation methods for $0 \leqslant \alpha \leqslant 4$; their results indicated lift can reach 17 at $\alpha = 4$ for a stationary cylinder, which also exceeds 4π. Karabelas and Koumroglou [15] investigated turbulent flow past a rotating cylinder at high Reynolds number and the results showed that lift coefficients are much smaller than those of Prandtl, even for rotation rate at 8; the lift was only around 5.5 because of the turbulent flow. For laminar flow at low Reynolds number, the results of Stojkovic and Breuer [10] indicated Prandtl's limit could be greatly exceeded and the trend for lift with increasing rotation rate is almost the same as that of Mittal and Kumar [11].

The other intriguing question is whether the *St* (Strouhal number for vortex shedding) increases with the increase of rotation rate and when does the Von Karman vortex street disappear. Diaz et al. [6] found that the Von Karman activity in the wake deteriorates and disappears at α in excess of 2 through an experiment at $Re = 9000$. Coutanceau and Menard [7] discovered only one vortex shed from the cylinder beyond a critical rotation rate and the critical rotation rate is almost independent of *Re* and is about 2. Chen et al. [8] observed that more than one vortex shed for $\alpha = 2$ and 3.25 at $Re = 200$, which is contrary to the earlier findings. They also found that the vortices shed later are much weaker than the ones shed initially and concluded that the rotation of the cylinder does not suppress vortex shedding for $Re = 200$ at $\alpha = 3.25$. Chew and Cheng [9] investigated the complex flow of a rotating cylinder at $Re = 1000$ using a hybrid vortex scheme, the periodic vortex shedding remained and formed a Karman vortex in the wake at $\alpha \leqslant 2$. They surmised that the exact behavior is sensitive to the value of α in the region $2 < \alpha < 3$ and it is difficult to obtain a critical value of α wherein the Karman vortex street completely disappears. Stojkovic et al. [10] confirmed that the existence of vortex shedding for $Re = 100$ at $0 \leqslant \alpha \leqslant 1.8$ and observed that the Karman vortex vanish at $\alpha > 1.8$, while a second shedding mode was found for the region $4.8 \leqslant \alpha \leqslant 5.15$; the second vortex shedding model was also supported by Mittal and Kumar [11] and Pralits et al. [12]. Results for the relationship of *St* with rotation rate are shown in Fig. 2. The results of Diaz et al. [6] and Chew and Cheng [9] show increases in *St* with increasing rotation rate and are supported by researchers such as Jaminet and Van Atta [16], Mittal and Kumar [11], Kumar and Cantu [17] and Kang and Choi [18] found that *St* decreases with increasingα.

Most of the mean lift coefficients at the large rotation rates presented in Fig. 1 are based on simulation methods. Banafsheh and Yahya [19] designed an experimental setup to investigate the wake distribution and hydrodynamics of a rotating cylinder for cross flow direction based on different rotation rates and reduced velocities, while the rotation rates were limited to 0–2.6. How does the lift coefficient vary with increasing rotation rate at large values, whether the Prandtl's limit can be exceeded, whether *St* increases with increasing rotation rate and when does the Von Karman vortex street disappear? To address these problems, a large rotation rate range from 0 to 8 was used experimentally in the current work. Additionally, Mittal [20] mentioned that the hydrodynamics strongly depend on the aspect ratio of the cylinders in three-dimensional simulation. The relationship between the hydrodynamics and aspect ratios is illustrated by the results of these experiments.

2 Experimental setup

The experiments were conducted in the circulating water channel at the Chiba Experiment Station of the University of Tokyo (length 25 m, width 1.8 m and maximum depth about 2 m), the water depth of the experimental area was 1.075 m. The velocity of the flow was controllable with variation of 0.3–1.0 m/s. Four replaceable cylinders with the same length $L = 0.59$ m, but different diameters (0.319, 0.267, 0.216 and 0.102 m) were tested (Fig. 3b). The cylinders were linked with the shaft by bolts and rotation of the shaft was controlled by an electric motor through a gear installed inside the system. The reduction ratio of the gear was 3:1 and the motor had a variable rotation speed in a range of 0–500 rpm. The cylinder controlled by the motor could be rotated clockwise or counter-clockwise and a torque meter (UNPULSE, TM300) was used to record the torque, speed and power of the motor. A six-axis force sensor installed in the system was used to measure the forces and moments for the six degrees of freedom (F_x, F_y, F_z, M_x, M_y, M_z). The schematic of the system is shown in Fig. 3a, the hollow cylinders were made from steel and the thickness of cylinder wall was 0.005 m. When the cylinders were immersed in water, the inside of the cylinders was filled with water. The round plates were used to weaken end effect of the cylinders and diameter and thickness of the two were 0.5 and 0.005 m, respectively. The cylinder was cantilevered and almost fixed, which was different from the experiment of Banafsheh and Yahya [19], where the cylinder could move at the cross flow direction.

Impact experiments were used to obtain the natural frequencies of different cylinders in the still water, Fig. 4 shows the first order natural frequency increased with

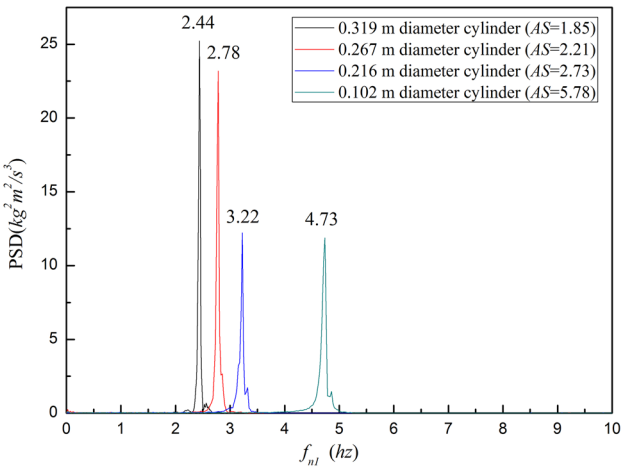

Fig. 4 First order natural frequencies, f_{n1}, of the four cylinders from impact experiment

Fig. 3 **a** Schematics of experiment setup. **b** Four different diameter cylinders. **c** Generated forces of rotating cylinders in flow

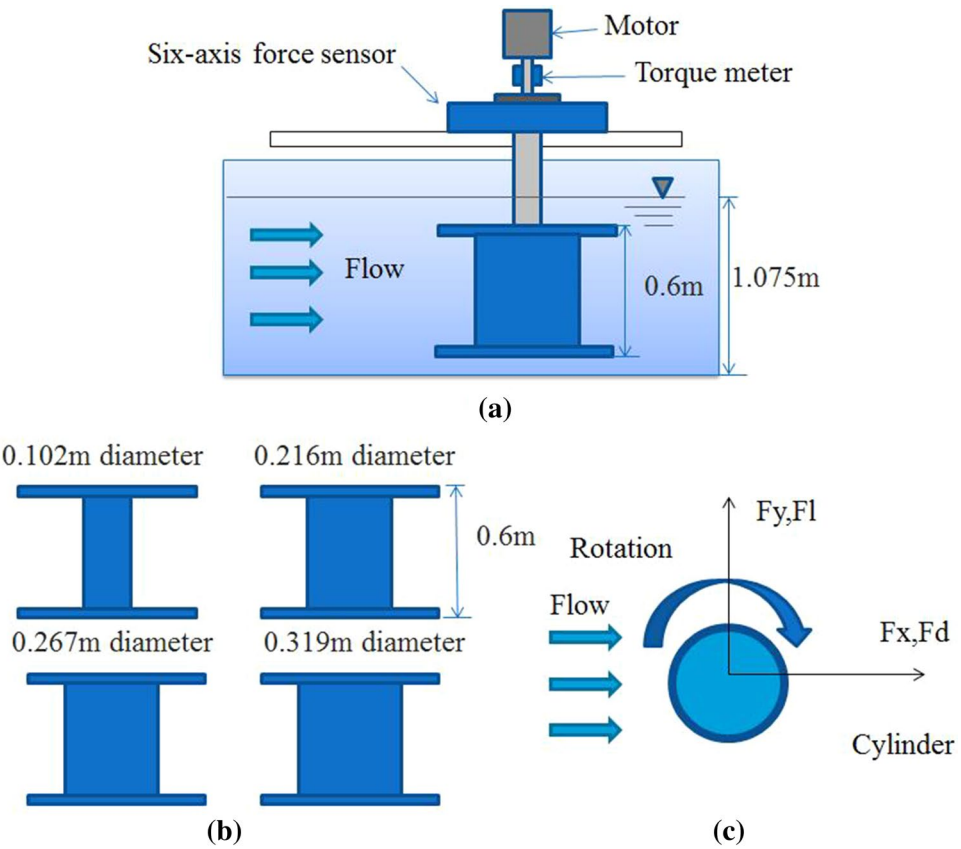

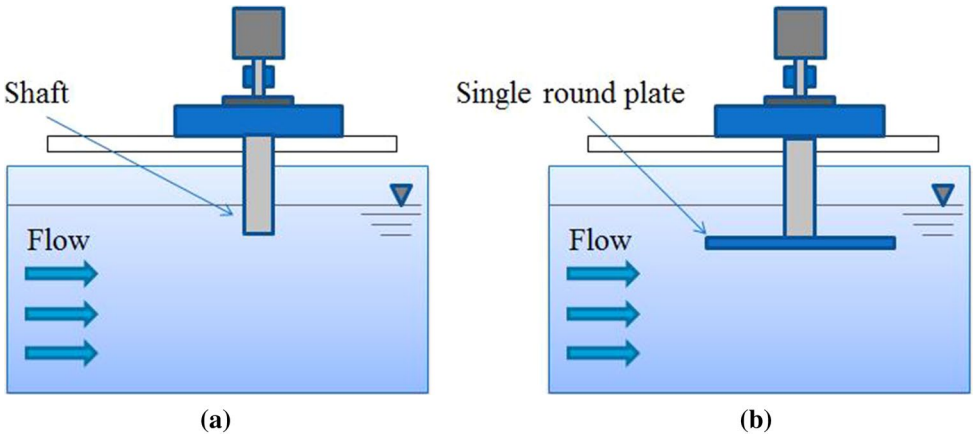

Fig. 5 **a** Shaft condition and **b** single round plate condition

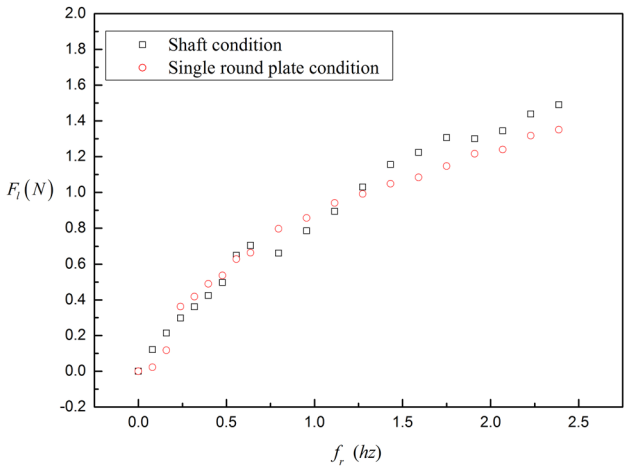

Fig. 6 Force at cross flow direction, F_1, of shaft condition and single round plate condition versus rotation frequencies, f_r, at flow velocity 0.3 m/s

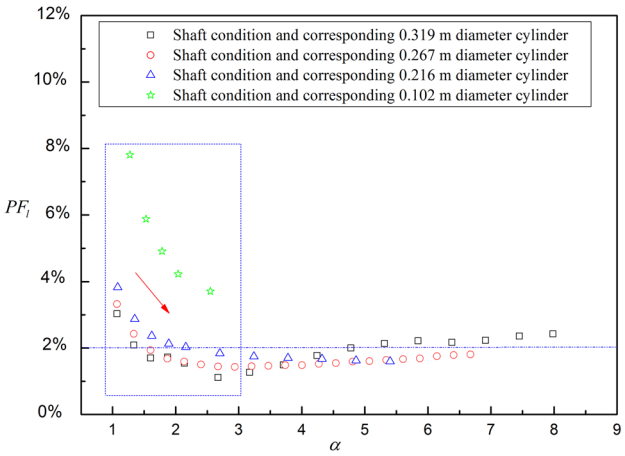

Fig. 7 Percentage of force at cross flow direction for shaft condition and the corresponding cylinders, $PF_1 = F_1(\text{shaft})/F_1(\text{cylinder})$, versus rotation rate, α, at flow velocity 0.3 m/s

decrease in cylinder diameter, the corresponding period can be described by the following equation:

$$T_1 = \frac{1}{f_{n1}}, \tag{1}$$

where f_{n1} is the first order natural frequency of the cylinders in the still water.

As shown in Fig. 3a, part of the shaft was immersed in water and round plates were attached to the cylinders. Taking these into consideration, the shaft condition and the single round plate condition were experimentally evaluated for different flow velocities and rotating frequencies. The setups for these conditions are shown in Fig. 5a, b.

Figure 6 shows the force at cross flow direction, F_1, for shaft condition and single round plate condition based on different rotation frequencies at flow velocity 0.3 m/s. F_1 increased with increasing rotation frequency and the results of the two conditions did not differ very much, which means that the round plates have little effect on the system. Percentage of force at cross flow direction for shaft only condition and the corresponding cylinder condition, $PF_1 = F_1(\text{shaft})/F_1(\text{cylinder})$, based on different rotation rates at flow velocity 0.3 m/s are shown in Fig. 7, PF_1 dramatically decreased at the rotation rate range from 1.0 to 3.0. When the rotation rate was larger than 3.0, the values of PF_1 for different cylinders remained around 2%. Thus, compared with the hydrodynamics of the rotating cylinder in flow, the contribution of the shaft and round plate to the hydrodynamics of the rotating cylinders is little. Absolutely, the effect of the shaft and round plate has been removed from the relevant forces for the cylinder described in the following sections.

3 Cylinder in flow (without rotation)

To understand the hydrodynamics that are generated on the cylinder because of the vortex shedding at the two sides of the cylinder, a series of tests were conducted for different cylinders in the flow velocity range from 0.3 to 1.0 m/s. The relevant lift coefficient, drag coefficient, Strouhal number and reduced velocity are described as following:

$$C_{\mathrm{l}} = \frac{F_{\mathrm{l}}}{\frac{1}{2}\rho DLU_{\infty}^{2}}, \tag{2}$$

$$C_{\mathrm{d}} = \frac{F_{\mathrm{d}}}{\frac{1}{2}\rho DLU_{\infty}^{2}} \tag{3}$$

$$s_{\mathrm{t}} = \frac{f_{\mathrm{v}}D}{U_{\infty}}, \tag{4}$$

$$U_{\mathrm{t}} = \frac{U_{\infty}}{f_{\mathrm{n}}D}, \tag{5}$$

where F_{l} and F_{d} are the forces at the cross flow direction and in-line direction, respectively, ρ is the density of water, D is the diameter of the cylinder, L is the length of the cylinder and U_{∞} is the flow velocity, f_{v} is the vortex shedding frequency, f_{n} is the natural frequency.

The time history of the lift coefficient, C_{l}, for the 0.319 m diameter cylinder at flow velocity 0.3 m/s is presented in Fig. 8 (this is the original data from the experimental observations without any data processing); as the vortexes are shedding from the cylinder, the periodical phenomenon of lift could be observed very clearly in Fig. 8.

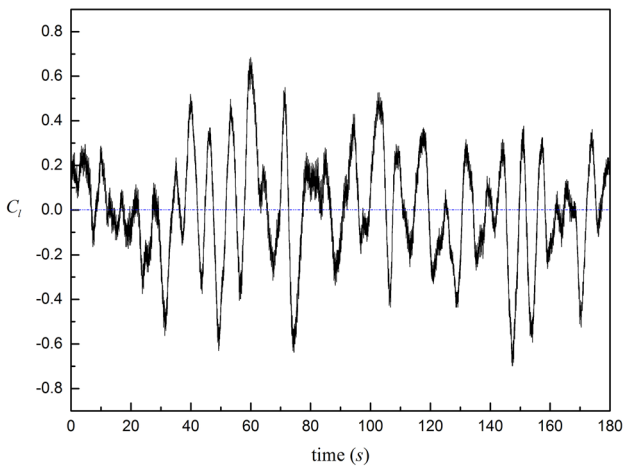

Fig. 8 Time history of the lift coefficient,C_{l}, for the 0.319 m cylinder at flow velocity 0.3 m/s (original experimental data)

3.1 Mean, frequency and root Mean square values for hydrodynamics

The Strouhal number, St, obtained from power spectrum of lift is plotted in Fig. 9a, to better describe the vortex shedding phenomenon ,two areas have been divided, the vortex shedding area for St (With only one value for Strouhal number, which means the vortex shedding regularly at only one period) was found at $9.5 \times 10^4 \leqslant Re \leqslant 1.5 \times 10^5$ and the values of St were around 0.15. For the weak vortex shedding area (Which means vortex shedding at one main period and several minor periods at this area) at $1.5 \times 10^5 \leqslant Re \leqslant 3.5 \times 10^5$, two or more values for St could be observed and values range increased as the increase of Re, even value of St at $Re = 3.0 \times 10^5$ equaled 0.38

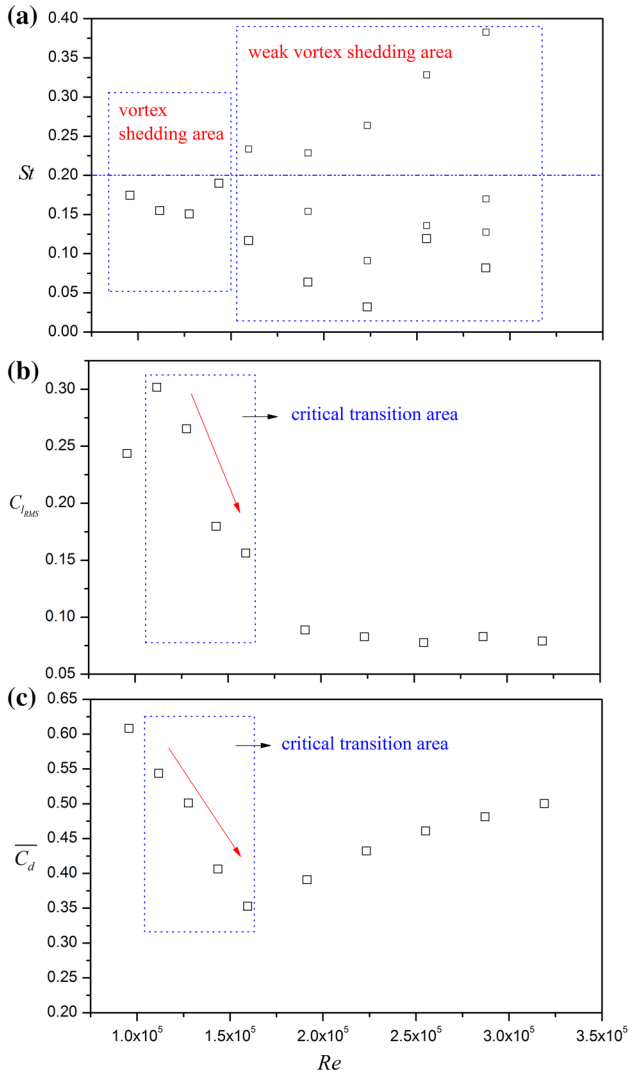

Fig. 9 **a** Strouhal number, St, **b** RMS values of lift force, $C_{\mathrm{l_{RMS}}}$, **c** mean drag coefficient, $\overline{C_{\mathrm{d}}}$, for 0.319 m diameter cylinder versus Reynolds number, Re

could be observed. As plotted in Fig. 9(b), values of Root Mean Square, RMS, for lift coefficient decreased at range $1.0 \times 10^5 \leqslant Re \leqslant 1.59 \times 10^5$ and then remained around 0.025 from $Re \geqslant 1.59 \times 10^5$. Similar decreased phenomenon of C_d at range $9.5 \times 10^4 \leqslant Re \leqslant 1.59 \times 10^5$could be observed in Fig. 9c. All of these indicate that critical transition area for 0.319 m cylinder is at $1.0 \times 10^5 \leqslant Re \leqslant 1.59 \times 10^5$, which is a little smaller than that of Gunter Schewe [21].

Many researchers have focused on the lock-in phenomenon when reduced velocity, U_r, is around 5 and obtained a series of investigation results, such as Feng [1]. In the current experiment, the maximum value of U_r was only two for the 0.102 m diameter cylinder at the largest flow velocity 1.0 m/s; even for this condition, little oscillation of the cylinder could be observed, which means the cylinders are close to the fixed model. The means of the drag coefficients, $\overline{C_d}$, for the different cylinders at different Reynolds number are shown in Fig. 10, for the 0.102 m diameter cylinder with the aspect ratio 5.78, which is the closest to the two-dimensional theoretical model compared to the other three cylinders and this resulted in the $\overline{C_d}$ for the 0.102 m diameter cylinder were much larger than those of the other two cylinders, the values of $\overline{C_d}$ for the 0.102 m diameter cylinder at $2.10^4 \leqslant Re \leqslant 10^5$ remained around 1.2 and those are close to the results of Blevins's experiment at $Re = 10^5$ [22, 23].For the critical transition area at $1.0 \times 10^5 \leqslant Re \leqslant 1.59 \times 10^5$, as the decreased phenomenon for 0.319 m diameter cylinder described in Fig. 9c, the similar decreased phenomenon of $\overline{C_d}$ for the 0.216 m cylinders could be observed.

Figure 11a shows Strouhal numbers, *St*, of the vortex shedding for different cylinders versus Reynolds number, same as the 0.319 m diameter cylinder in Fig. 9a. The vortex shedding weakened at the critical transition area $1.0 \times 10^5 \leqslant Re \leqslant 1.59 \times 10^5$. For the 0.102 m diameter cylinder, the values of *St* were around 1.90 at $Re \leqslant 10^5$, which are close to the those of Blevins's experiment at $Re=10^5$ [22, 23].Values of *St* for the other two cylinders were a little smaller than those of 0.102 m diameter cylinder. RMS values of the lift coefficient, $C_{l_{RMS}}$, for the cylinders are shown in Fig. 11b. For the 0.102 m diameter cylinder, the $C_{l_{RMS}}$ were around 0.45 at $2 \times 10^4 \leqslant Re \leqslant 10^5$, which were close to the experiment results of Dong and Karniadakis [24] at $Re \approx 10^4$. The $C_{l_{RMS}}$ for this cylinder were much larger than for the other two cylinders and the reason maybe the same as for $\overline{C_d}$shown in Fig. 10. A decreasing phenomenon of $C_{l_{RMS}}$

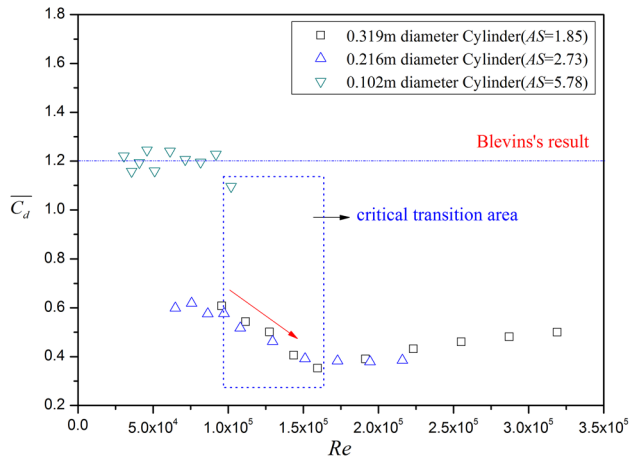

Fig. 10 Mean values of drag coefficient, $\overline{C_d}$, for different cylinders versus the Reynolds number, *Re*.(The experiment data of 0.267 m diameter cylinder were not plotted here, as the 0.102, 0.216 and 0.319 m diameter cylinders were manufactured at the first time at Oct, 2015 and 0.267 m diameter cylinder were manufactured at the second time at Feb 2016, which is the added cylinder used to perfected the blank between the 0.319 m diameter cylinder and 0.216 m diameter cylinder, and the experimental data of 0.267 m diameter cylinder in flow was a little unreliable because of slight surface roughness of the secondary manufacture, the same reason for Fig. 11)

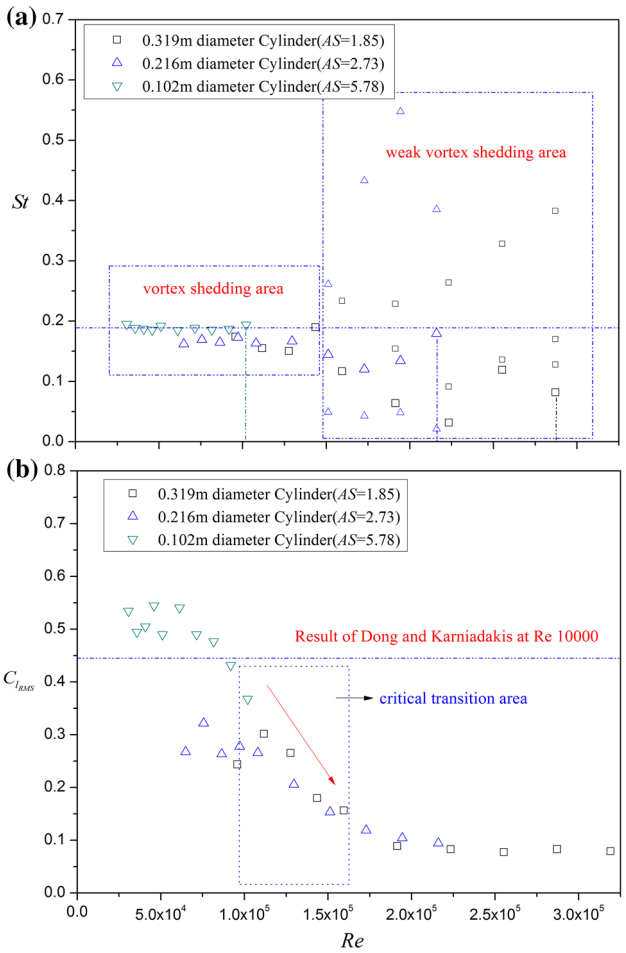

Fig. 11 **a** Strouhal number, *St*, **b** RMS values of lift force, $C_{l_{RMS}}$, for the cylinders at regular area versus Reynolds number, *Re* (the vertical dashed line is the maximum *Re* for the cylinders, respectively, which is limited by the flow range from 0.3 to 1.0 m/s)

for the three cylinders could be observed around the critical transition area ($1.0 \times 10^5 \leqslant Re \leqslant 1.59 \times 10^5$) in Fig. 11b.

4 Rotating cylinder in flow

As shown in Fig. 3c, lift force is generated in the cross flow direction when the rotating cylinder in the flow, and there are several confusions related to the mean lift coefficient presented in Fig. 1, including whether the Prandtl's limit can be exceeded, how the lift coefficient changes with the increase of rotation rate at high rotation rate and the relationship between the maximum lift coefficient and aspect ratio of the cylinder [10, 11, 13–17]. To shed some light on these issues, experiments were conducted at flow velocities of 0.3, 0.5 and 0.7 m/s with rotation frequencies from 0 to 2.38 Hz, and relevant hydrodynamics of the cylinders have been analyzed. Figure 12a shows the time history of the detected forces at cross flow direction (including inertial component and hydrodynamics component) for the 0.319 m cylinder at rotation frequency 1.59 Hz for 0.3 m/s velocity flow. The inertial component is generated by the centrifugal movement, which was depended on the relationship of self-rotation frequency of the cylinder and the natural frequency of the cylinder; the frequency of inertial component is the same as the rotation frequency, as shown in Fig. 12b. While the hydrodynamics component is concerned with the vortex shedding, in the present paper, the inertial forces were removed and all of the forces discussed below are the hydrodynamic components. Lift force and drag force (hydrodynamics) can be described by the following equation and the relevant force coefficients are described by Eqs. (2) and (3).

$$F_l(t) = F_{my}(t) - F_{iy}(t) \quad F_d(t) = F_{mx}(t) - F_{ix}(t), \tag{6}$$

where $F_l(t)$ is the lift force and $F(t)$ is the drag force, $F_{mx}(t)$ and $F_{my}(t)$ are the measured forces for cross flow and in-line directions,$F_{ix}(t)$ and $F_{iy}(t)$ are the inertial forces for cross flow and in-line directions.

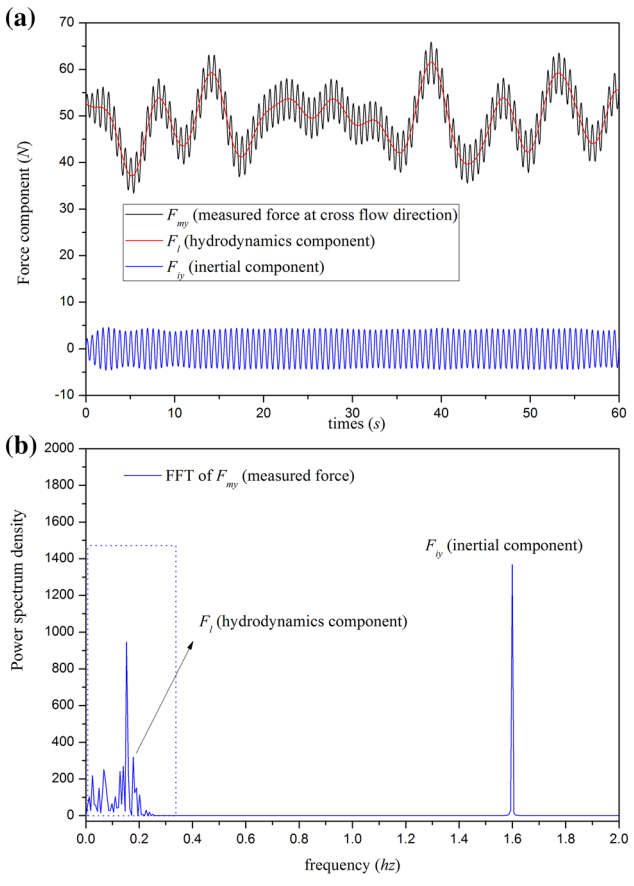

Fig. 12 Time history (**a**) and FFT components **b** of the forces for 0.319 m diameter cylinder at rotation frequency 1.59 Hz at flow velocity 0.3 m/s

4.1 Mean hydrodynamics coefficients for rotating cylinders in flow

Based on Eqs. (2) and (3), the time histories of the lift coefficient, C_l, and drag coefficient, C_d, (hydrodynamics) of the 0.319 m cylinder at different rotation rates at the flow velocity 0.3 m/s are shown in Fig. 13. The rotation rates 0.53, 2.14, and 6.38 correspond to the initial area, increasing area and equivalent area in Fig. 14a, the mean drag was larger than mean lift at rotation rate 0.53, but then lift dramatically increased and even became much larger than drag, the mean lift was around 5.2 at rotation rate 2.14 and at where the mean drag was around 2.75. Finally at rotation rate 6.38 in the equivalent area, the mean value of lift was around 6.62 and the mean value of drag dramatically increased to 7.38, which are close to each other. The FFT results of lift and drag are shown in Fig. 14b, the amplitude of power spectrum density for lift was much larger than that for the drag at rotation rate 0.53, and then remained almost the same at rotation rate 2.14 and 6.38 as the increase of rotation rate.

The mean values of the hydrodynamics coefficient, $\overline{C_d}$ and $\overline{C_l}$, of the 0.319 m diameter cylinder at flow velocity 0.3 m/s are shown in Fig. 14(a). As the rotation rate increased, $\overline{C_l}$ dramatically increased, which explains why the PF_l (in Fig. 7) dramatically decreased in the rotation range from 1.0 to 3.0, and then became constant when the rotation rate was close to 3.0. $\overline{C_d}$ initially decreased slightly with increase in rotation rate and then increased rapidly and finally increased slowly from a rotation rate around 4, the initial decreasing phenomenon of $\overline{C_d}$were observed by a lot of researchers [11, 14], while the discussion for the current new finding that $\overline{C_d}$ would increase and then even larger than $\overline{C_l}$ at larger rotation rate was little. Based on the variation of the mean lift coefficient and mean drag coefficient, three areas

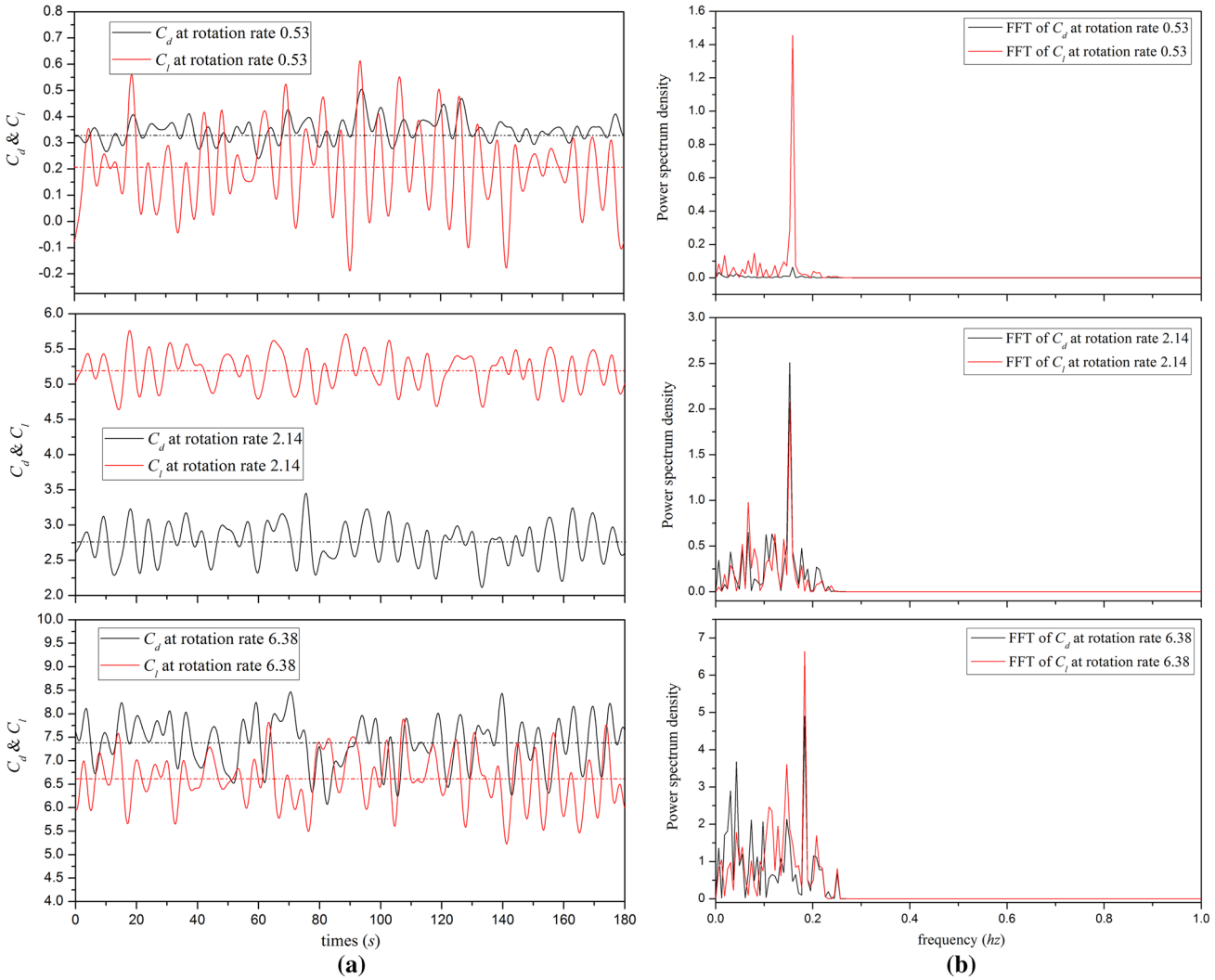

Fig. 13 **a** Times history and **b** FFT of lift coefficient, C_l, and drag coefficient, C_d, (hydrodynamics) of 0.319 m cylinder at different rotation rates at the flow velocity 0.3 m/s

were defined to describe this, (a) initial area(which indicates at the initial stage): at where $\overline{C_d}$ decreased slightly and $\overline{C_l}$ increased slightly; (b) increasing area(which means values dramatically increased at this area): at where $\overline{C_d}$ and $\overline{C_l}$ were dramatically increasing and values of $\overline{C_l}$ were larger than $\overline{C_d}$; (c) equivalent area(which manifests values closed to others at this area): at where $\overline{C_l}$ remained constant, the values of $\overline{C_d}$ and $\overline{C_l}$are close to each other and where $\overline{C_d}$ is a little larger than $\overline{C_l}$. Combined with those defined areas of the other three cylinders plotted in Fig. 14b–d, the range of initial area for the 0.102 m diameter cylinder was at $0 \leqslant \alpha \leqslant 1.07$, which was a littler larger than that of the other three. however, the range of increasing area dramatically increased as the increase of the aspect ratio (though the maximums of rotation rates for 0.216 m cylinder and 0.102 m cylinder were limited by motor range 0–500 rpm, the growth trend of increasing area could be inferred).The mean resultant force coefficient, $\overline{C_r}$, (combination of the lift and drag) and the relevant angle between the resultant force and in-line direction versus rotation rate are shown in Fig. 15. The variation trends for $\overline{C_r}$ were similar to $\overline{C_d}$ and the maximum for $\overline{C_r}$ was around 10. The angle initially increased dramatically with increasing rotation rate and approached 70 degrees at the rotation rate range from 1.0 to 2.0. Corresponding the increasing area shown in Fig. 14a, this was a result of the values of $\overline{C_l}$ being much larger than $\overline{C_d}$ at this area. The angle then decreased at higher rotation rates and finally remained around 45 degrees, which indicates that the $\overline{C_l}$ and $\overline{C_d}$ were very close, as the equivalent area shown in Fig. 14a.

Figure 16a shows the mean values of the drag coefficient, $\overline{C_d}$, for different cylinders; As the 0.319 m diameter cylinder described in Fig. 14a, the same decreasing phenomenon could be observed for other three cylinders at initial area. The growth rate of increasing area for $\overline{C_d}$ decreased

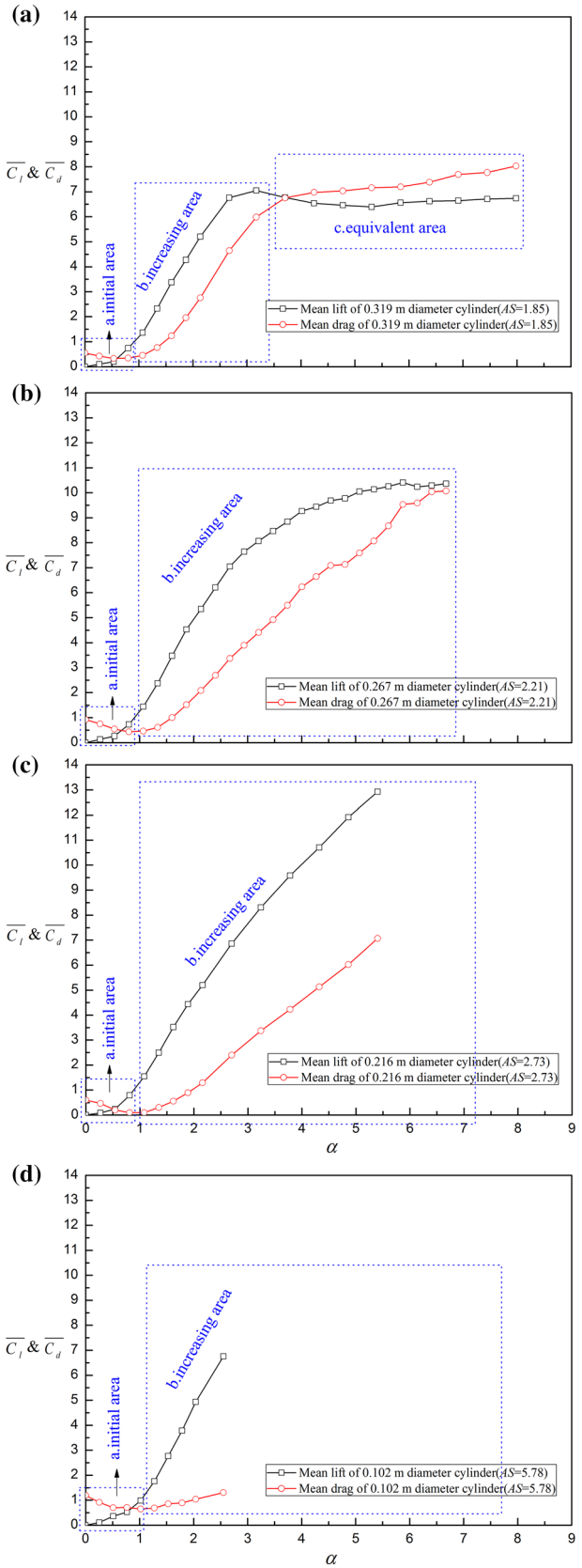

Fig. 14 The mean values of the hydrodynamics coefficient, $\overline{C_d}$ and $\overline{C_l}$, of the cylinders at flow velocity 0.3 m/s versus rotation rate, α

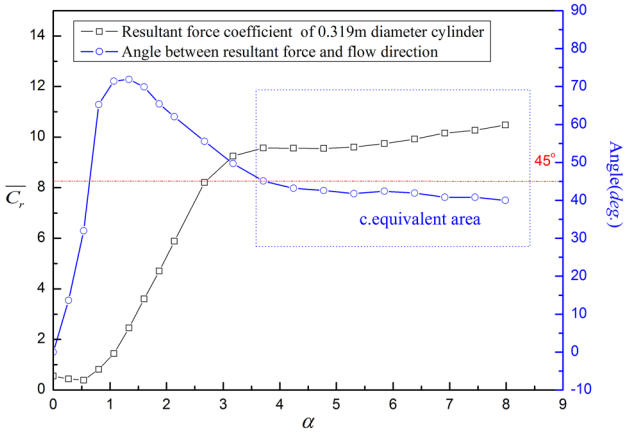

Fig. 15 The mean of the resultant force coefficient, $\overline{C_r}$, and the angle between the resultant force coefficient and flow direction for the 0.319 m diameter cylinder versus rotation rate, α

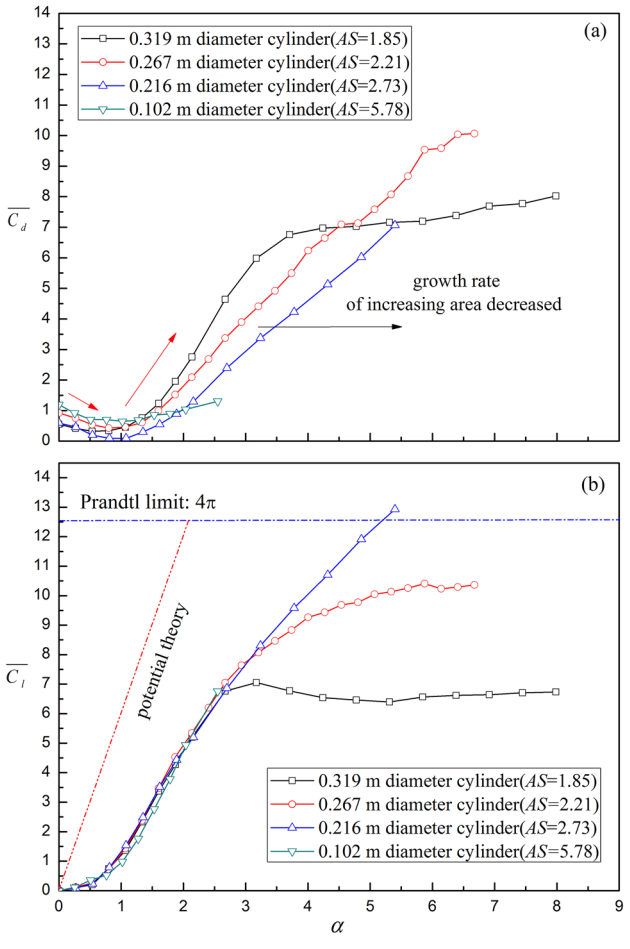

Fig. 16 (a) The means of the drag coefficient, $\overline{C_d}$, and **b** lift coefficient, $\overline{C_l}$, for different cylinders at flow velocity 0.3 m/s versus rotation rate, α

as the increase of aspect ratio. As the variation trends, the $\overline{C_d}$ at equivalent area for the cylinders would increase as the increase of aspect ratio (Though the values of 0.216 m diameter cylinder and 0.102 m diameter cylinder at large rotation rate were limited by the range of motor at 0–500 rpm, the variation trends could be estimated). The mean values of the lift coefficient, $\overline{C_l}$, for different cylinders are shown in Fig. 16b; compared to the results of potential theory, the $\overline{C_l}$ for different cylinders were much smaller and almost the same when rotation rate was less than 2.67. At higher rotation rates, the $\overline{C_l}$ for the different cylinders gradually diverge and became different constant values at different rotations rates. The constant values for hydrodynamic parameters and the rotation rates for the inflection points were strongly dependent on the aspect ratio of the cylinders, which affected the wake three-dimensionality and then changed the hydrodynamic of the cylinder [20]. As shown in Fig. 1 that whether the limit of Prandtl can be exceeded, the maximum rotation rates for different cylinders are limited by the range of the motor (range at 0–500 rpm), even though the $\overline{C_l}$ for the 0.216 m diameter cylinder at rotation rate 5.4 was 13.0; a little larger than the limit of Prandtl, the results of the current experiment does not completely support the conclusion that Prandtl's limit can be exceeded. While, based on the variation trends, the assumption that the lift of 0.102 m diameter cylinder will exceed the Prandtl's limit if the rotation rate large enough is supported by this current work.

4.2 Strouhal number and RMS values of lift coefficient for the rotating cylinders in flow

The Frequencies of lift coefficient, C_l,of 0.319 m diameter cylinders at flow velocity 0.3 m/s versus the rotation rate are shown in Fig. 17,Based on the different wake formation and the previous research achievement [6–12, 16–18], three areas were divided, the definition of vortex shedding area and weak vortex shedding area were similar to those in Figs. 9a and 11a, for the vortex shedding area and weak vortex shedding area, such as the FFT result of at rotation rate 0.53 and 2.14 in Fig. 13b, one clear peak frequency could be observed. For the wake fluctuation area, frequencies of lift coefficient would be at a range instead of those concentrated at one or two values, such as the FFT result of $\overline{C_l}$ at rotation rate 6.0 in Fig. 13b, and the reason for the existence of these frequencies is considered because of the unsteady wake fluctuation, which is different from the vortex shedding at rotation rate smaller than 3.0 [6–12]. One need to notice that the range of the three areas is decided by rotation rate, which is different from those three areas for mean hydrodynamics(initial, increasing and equivalent areas) that decided by rotation rate and aspect ratio.

Based on the description for Strouhal number, St, in Eq. (4), St for the four cylinders at various rotation rates at flow velocity 0.3 m/s are shown in Fig. 18a. At the vortex shedding area, the values of St were a little increase as the increase of rotation rates, for the 0.102 m diameter cylinder

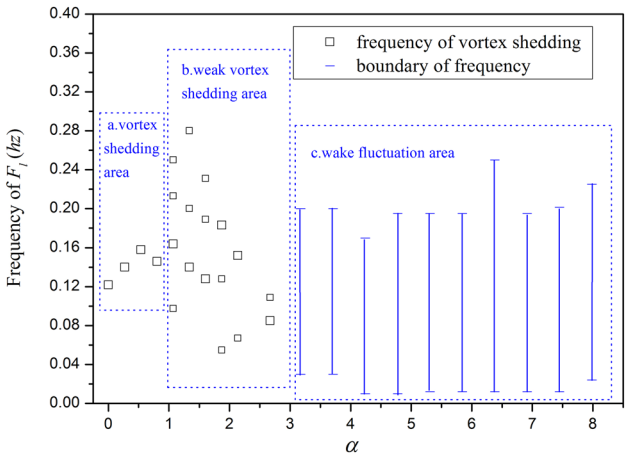

Fig. 17 Frequencies of lift coefficient, C_l, of 0.319 m diameter cylinders at flow velocity 0.3 m/s versus the rotation rate, α

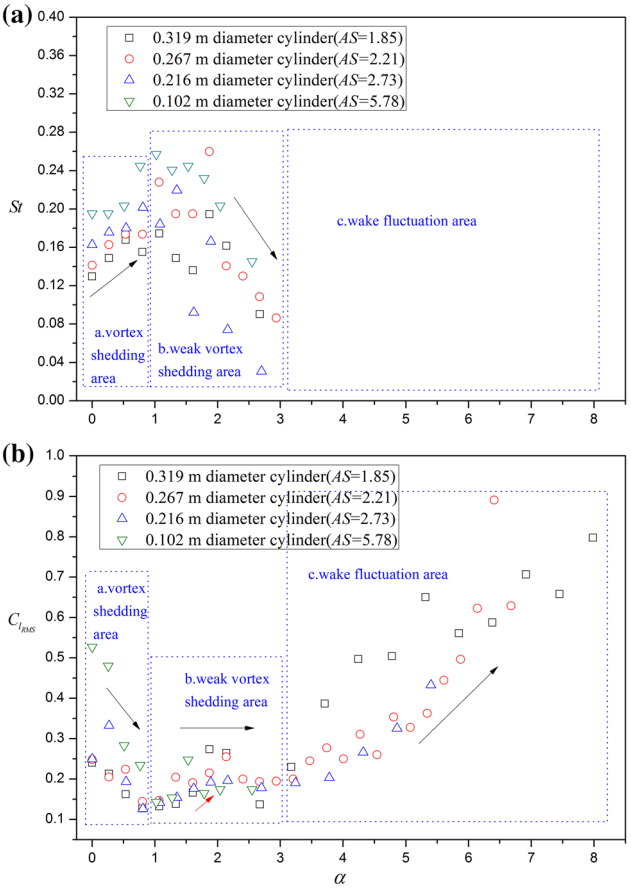

Fig. 18 **a** The Strouhal number, St, and **b** the RMS values of lift coefficient, $C_{l_{RMS}}$, of 0.267, 0.216 and 0.102 m diameter cylinders at flow velocity 0.3 m/s versus the rotation rate, α

with 5.78 aspect ratio, the values of *St* were a little larger than those of the other three cylinders. Then the *St* decreased and disappeared at range $1.75 \leqslant \alpha \leqslant 3.25$, which is in agreement with the results of previous researchers [6–12]. As shown in Fig. 2, disagreement still existed for the question that whether *St* increases with increasing rotation rate. The initial increasing and then decreasing phenomenon for the four cylinders is similar to the experiment results of Kumar and Cantu [17], in which *St* did exist in the rotation rate range from 0.0 to 2.0 and reappeared in the range from 4.34 to 4.70. However, reappearance of *St* was not observed for the cylinders in the current experiments.

Figure 18b shows the RMS values of lift coefficient, $C_{l_{RMS}}$, for the four cylinders, at the vortex shedding area, the $C_{l_{RMS}}$ decreased as the increase of rotation rates (This means that energy of vortex shedding has been weakened by the rotation) and the $C_{l_{RMS}}$ for 0.102 m diameter cylinder with AS = 5.78 were much larger than those of the other three cylinders, the reason maybe the same as for $\overline{C_d}$ shown in Fig. 10 and the $C_{l_{RMS}}$ shown in Fig. 11b that the 0.102 m diameter cylinder with AS = 5.78 is closest to the two-dimensional model. At the weak vortex shedding area, the $C_{l_{RMS}}$remained steady and a littler heave could be observed at $\alpha \approx 2.0$, the reason maybe the vortex formation has been changed because the shedding frequency dramatically decreased at $\alpha \approx 2.0$. As the rotation rate increased, vortex shedding would disappear and wake fluctuation started, which would induce the $C_{l_{RMS}}$ increased as the increase of rotation rate.

4.3 Discussion of Reynolds number effect

Figure 19 shows the mean lift and drag coefficients, $\overline{C_d}$ and $\overline{C_l}$, for the 0.319 m diameter cylinder versus rotation rates at three different Reynolds numbers (range $9.6 \times 10^4 \leqslant Re \leqslant 2.23 \times 10^5$), corresponding to flow velocity 0.3 m/s,0.5 m/s and 0.7 m/s; a little difference of $\overline{C_l}$ and $\overline{C_d}$ at initiation could be observed and then values and variation tendency for $\overline{C_l}$and $\overline{C_d}$ were almost the same as the increase of rotation rates, which indicates that $\overline{C_l}$and $\overline{C_d}$ mainly depends on the rotation rate and the Reynolds number does not have much influence on mean hydrodynamics at range $9.57 \times 10^4 \leqslant Re \leqslant 2.23 \times 10^5$. Combining the results of $\overline{C_l}$ and $\overline{C_d}$ at $3.06 \times 10^4 \leqslant Re \leqslant 9.57 \times 10^4$ in Fig. 16a, b, the conclusion that Reynolds number at range $3.06 \cdot 10^4 \leqslant \mathrm{Re} \leqslant 2.23 \cdot 10^5$has no much influence on the mean hydrodynamics (mainly depend on the rotation rate) could be obtained. For the 0.102 m diameter cylinder which is closest to the two-dimensional model, the Strouhal number, *St*, at two different Reynolds numbers for different rotation rates is shown in Fig. 20. The values for *St* and the variation trends was almost the same for the two Reynolds numbers, which indicates that *St* is strongly dependent on the

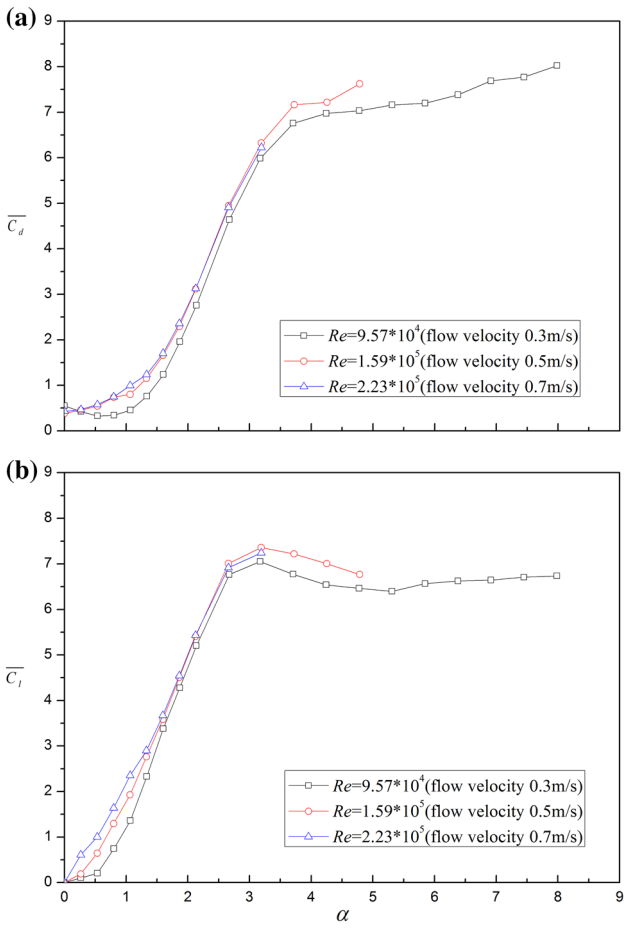

Fig. 19 **a** The drag coefficient, C_d, and **b** lift coefficient, C_l, for 0.319 m diameter cylinder at different Reynolds number versus rotation rate, α

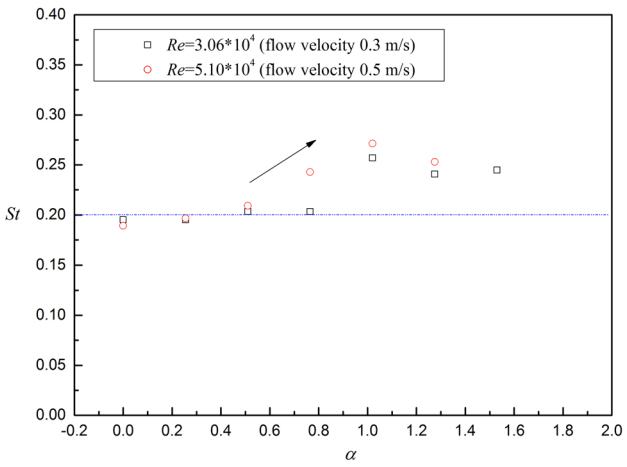

Fig. 20 The Strouhal number, *St*, of 0.102 m diameter cylinder at two different Reynolds numbers versus the rotation rates, α

rotation rate and weakly dependent on the Reynolds number at range $3.06 \times 10^4 \leqslant Re \leqslant 5.10 \times 10^4$.

5 Conclusions

A series of experiments were conducted to study the hydrodynamics of cylinders and rotating cylinders in flow. Two main significant issues were addressed in this paper; the first was how the hydrodynamics varied at high rotation rates for rotating cylinder in flow, The other was whether the aspect ratio as a vital parameter that dramatically influenced the hydrodynamics of the cylinder.

For the cylinders in flow condition, the critical transition area for cylinders at $1.0 \times 10^5 \leqslant Re \leqslant 1.59 \times 10^5$ has been confirmed. At the critical transition area, the vortex shedding weakened, mean drag coefficient and RMS values of life coefficient dramatically decreased. Compared with the other two cylinders, the 0.102 m diameter cylinder with AS = 5.78 was closest to the two-dimensional theoretical model, the results for this cylinder were much larger than those of the other three and much closer to two-dimensional results of other researchers.

For the rotating cylinders in flow, Variation of mean of hydrodynamics is considered decided by rotation rate and aspect ratio. Initial area, increasing area and equivalent area were defined to describe the variation of mean hydrodynamics and ranges of these areas dramatically influenced by the aspect ratio. At initial area, $\overline{C_\mathrm{d}}$ decreased slightly and $\overline{C_\mathrm{l}}$ increased slightly. For the increasing area, the $\overline{C_\mathrm{d}}$ and $\overline{C_\mathrm{l}}$ were dramatically increasing while values of $\overline{C_\mathrm{l}}$ were larger than $\overline{C_\mathrm{d}}$. At the equivalent area the $\overline{C_l}$ remained constant, the values of $\overline{C_\mathrm{d}}$ and $\overline{C_\mathrm{l}}$ are close to each other and where $\overline{C_\mathrm{d}}$ is a little larger than $\overline{C_\mathrm{l}}$. Different from the mean hydrodynamics, Strouhal number (vortex shedding) and Root mean square of lift are regarded as only depended on the rotation rate. Based on the wake formation, vortex shedding area, weak vortex shedding area and wake fluctuation area were defined to explain the variation of RMS of lift. Especially, though vortex shedding would disappear at rotation rate larger than 3.0, RMS of lift (energy of vibration) would increase as the increase of rotation rate because of wake fluctuation.

Finally, discussion of the Reynolds number indicates that hydrodynamics of the cylinder are strongly dependent on the rotation rate and weakly dependent on Reynolds number. In conclusion, the aspect ratio and the rotation rate are two significant parameters on the hydrodynamics of the rotating cylinder in flow, if the two could be large enough; the argument that Prandtl's limit can be exceeded is supported by this current work.

Acknowledgements The authors are grateful to Mr. Zengo Yoshida, an researcher at Chiba Experiment Station of the University of Tokyo, for his enthusiastic help in setting up the experiments and to Mr. Robert Kawaratani for his careful help in proofreading this paper.

References

1. Feng CC (1968) MSC. Thesis, University of British Columbia, Vancouver, BC
2. Prandtl L (1925) The magnus effect and wind powered ships. Naturwissenschaften 13:93
3. Prandtl L, Tietjens OG (1934) Applied hydro- and aeromechanics. McGraw-Hill, New York
4. Swanson WM (1961) The Magnus effect: A summary of investigation to data. J Basic Eng 83:46
5. Chew YT (1987) Flow past a rotating cylinder. In: Proceedings of international conference on fluid mechanics, Beijing, China, 1987, Beijing University Press, pp 556–560
6. Diaz F, Gavalda J, Kawall JG, Keller JF, Giralt F (1983) Vortex shedding from a spinning cylinder. Phys Fluids 26:3454
7. Coutanceau M, Menard C (1985) Influence of rotation on the near-wake development behind an impulsively started circular cylinder. J Fluid Mech 158:399
8. Chen YM, Ou YR, Pearlstein AJ (1993) Development of the wake behind a circular cylinder impulsively started into rotary and rectilinear motion. J Fluid Mech 253:449
9. Chew YT, Cheng M, Luo SC (1995) A numerical study of flow past a rotating circular cylinder using a hybrid vortex scheme. J Fluid Mech 299:35
10. Stojkovic D, Breuer M, Durst F (2002) Effect of high rotation rates on the laminar flow around a circular cylinder. Phys Fluids 14:3160
11. Mittal S, Kumar B (2003) Flow past a rotating cylinder. J Fluid Mech 476:303
12. Pralits JO, Brandt L, Giannetti F (2010) Instability and sensitivity of the flow around a rotating circular cylinder. J Fluid Mech 650:513
13. Tokumaru PT, Domotakis PE (1993) The lift of a cylinder executing rotary motions in uniform flow. J Fluid Mech 255:1
14. Bourguet R, Jacono DL (2014) Flow-induced vibrations of a rotating cylinder. J Fluid Mech 740:342
15. Karabelas SJ, Koumroglou BC (2012) High Reynolds number turbulent flow past a rotating cylinder. Appl Math Model 36:379
16. Jaminet JF, Van Atta CW (1969) Experiments on vortex shedding from rotating circular cylinders. AIAA Paper No, pp 1969–5407
17. Kumar S, Cantu C (2011) Flow past a rotating cylinder at low and high rotation rates. J Fluids Eng 133:041201
18. Kang S, Choi H (1999) Laminar flow past a rotating cylinder. Phys Fluids 11:3312
19. Banafsheh SA, Yahya MS (2015) An experimental investigation of vortex-induced vibration of a rotating circular cylinder in the cross-flow direction. Phys Fluids 27:067101
20. Mittal S (2004) Three-dimensional instabilities in flow past a rotating cylinder. J Appl Mech 71:89
21. Schewe G (1983) On the force fluctuations acting on a circular cylinder in cross-flow from subcritical up to transcritical Reynolds numbers. Phys Fluids 133:265
22. Mustto AA, Gustavo Bodstein CR (2001) Improved vortex method for the simulation of the flow around circular cylinders (C). AIAA Paper No, pp 2001–2643
23. Blevins RD (1990) Flow induced vibrations, 2nd edn. Van Nostrand Reinhold Co., New York
24. Dong S, Karniadakis GE (2005) DNS of flow past a stationary and oscillating cylinder at $Re = 10000$. J Fluids Struct 20:519